Synthesis, Thermal Processing, and Thin Film Morphology of Poly(3-hexylthiophene)–Poly(styrene Sulfonate) Block Copolymers

Harikrishna Erothu,[1] Joanna Kolomanska,[1] Priscilla Johnston,[1] Stefan Schumann,[2] Dargie Deribew,[3] Daniel T. W. Toolan,[4] Alberto Gregori,[5] Christine Dagron-Lartigau,[5] Giuseppe Portale,[6] Wim Bras,[6] Thomas Arnold,[7] Andreas Distler,[3] Roger C. Hiorns,[8] Parvaneh Mokarian-Tabari,[9,10] Timothy W. Collins,[9] Jonathan R. Howse,[4] and Paul D. Topham[1*]

1. Chemical Engineering and Applied Chemistry, Aston University, Birmingham, B4 7ET, UK.

2. Heraeus Deutschland GmbH & Co. KG, Business Line Display and Semiconductors (HNB), Chempark Leverkusen / Gebäude B 202, D-51368 Leverkusen, Germany.

3. Belectric OPV GmbH, Landgrabenstr. 94, 90443 Nürnberg, Germany.

4. Department of Chemical and Process Engineering, University Of Sheffield, Sheffield, S1 3JD, UK.

5. Institut des Sciences Analytiques et de Physico-chimie pour l'Environnement et les Matériaux (IPREM) UMR 5254, Université de Pau et des Pays de l'Adour, 64053 Pau, France.

6. Netherlands Organisation for Scientific Research, DUBBLE@ESRF Beamline BM26, ESRF - The European Synchrotron, 71, Avenue des Martyrs, CS 40220, 38043, Grenoble Cedex 9, France.

7. I07 Beamline, Diamond Light Source Ltd, Harwell Science and Innovation Campus, Didcot, OX11 0DE, UK.

8. CNRS, Institut Pluridisciplinaire de Recherche sur l'Environment et les Materiaux (IPREM UMR 5254), 64053 Pau, France.

9. Department of Chemistry, University College Cork and Tyndall National Institute, Cork, Ireland.

10. Centre for Research on Adaptive Nanostructures and Nanodevices (CRANN) and AMBER Centre, Trinity College Dublin, Dublin, Ireland.

E-mail: p.d.topham@aston.ac.uk

Table S1. Reaction conditions for the synthesis of $PNSS_x$-N_3.

PNSS-N_3	**NSS [g, (mmol)]**	**AIBN [g, (mmol)]**	**CTA-N_3 [g, (mmol)]**	**Anisole (ml)**
$PNSS_9$-N_3	5.056 (19.6)	0.064 (0.393)	0.853 (1.96)	5
$PNSS_{16}$-N_3	6.001 (23.5)	0.038 (0.235)	0.511 (1.17)	6
$PNSS_{23}$-N_3	7.018 (27.5)	0.030 (0.183)	0.398 (0.93)	7

Table S2. Reaction conditions for the synthesized diblock copolymers, $P3HT_{50}$-*b*-$PNSS_x$.

$P3HT_{50}$-*b*-$PNSS_x$	**$P3HT_{50}$ [g, (mmol)]**	**PNSS-N_3 [g, (mmol)]**	**CuI [g, (mmol)]**	**DIPEA (ml)**
$P3HT_{50}$-*b*-$PNSS_9$	0.250 (0.03)	0.578 (0.180)	0.057 (0.299)	1
$P3HT_{50}$-*b*-$PNSS_{16}$	0.250 (0.03)	1.03 (0.180)	0.057 (0.299)	1
$P3HT_{50}$-*b*-$PNSS_{23}$	0.250 (0.03)	1.5 (0.180)	0.057 (0.299)	1

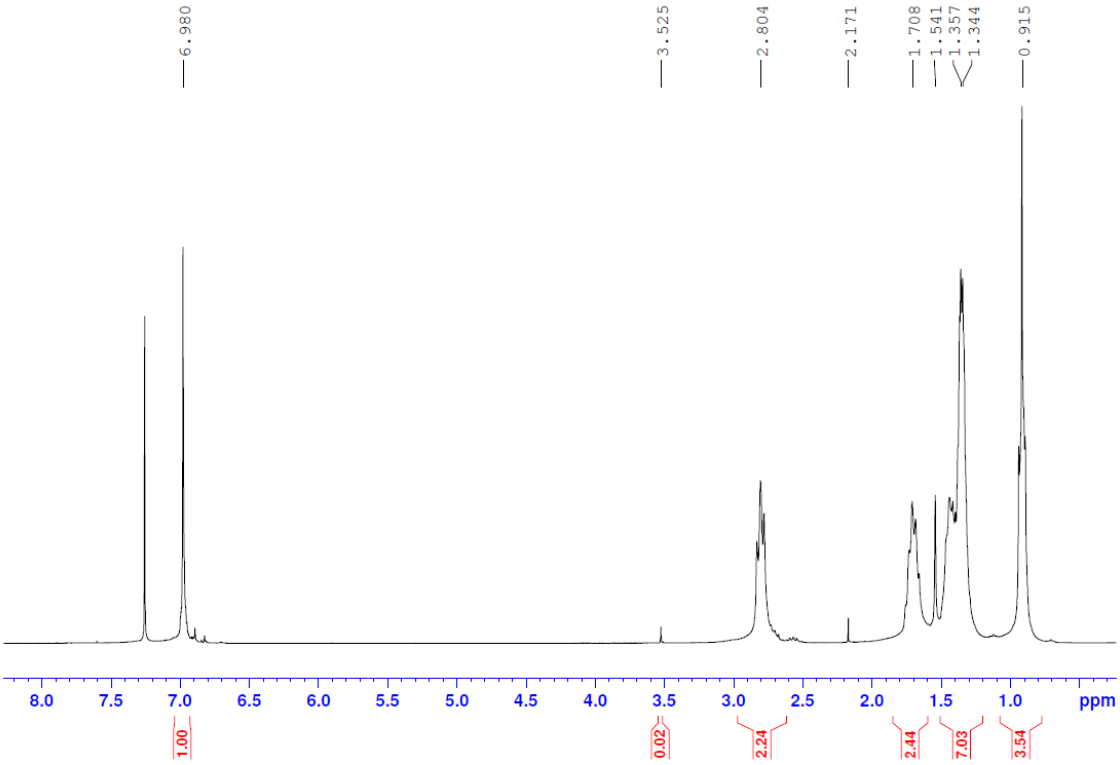

Figure S1. ^{1}H NMR spectrum of $P3HT_{50}$-ethynyl.

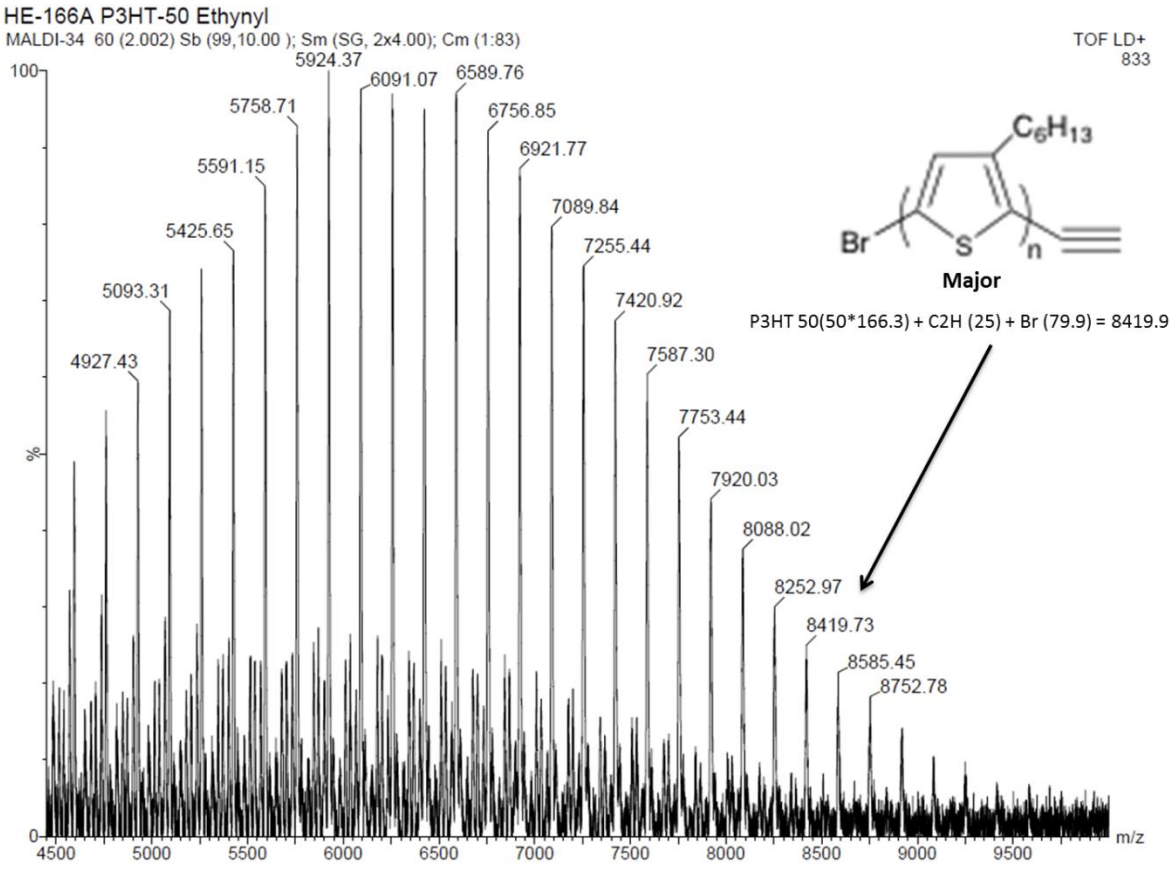

Figure S2. MALDI-ToF spectrum of $P3HT_{50}$-ethynyl.

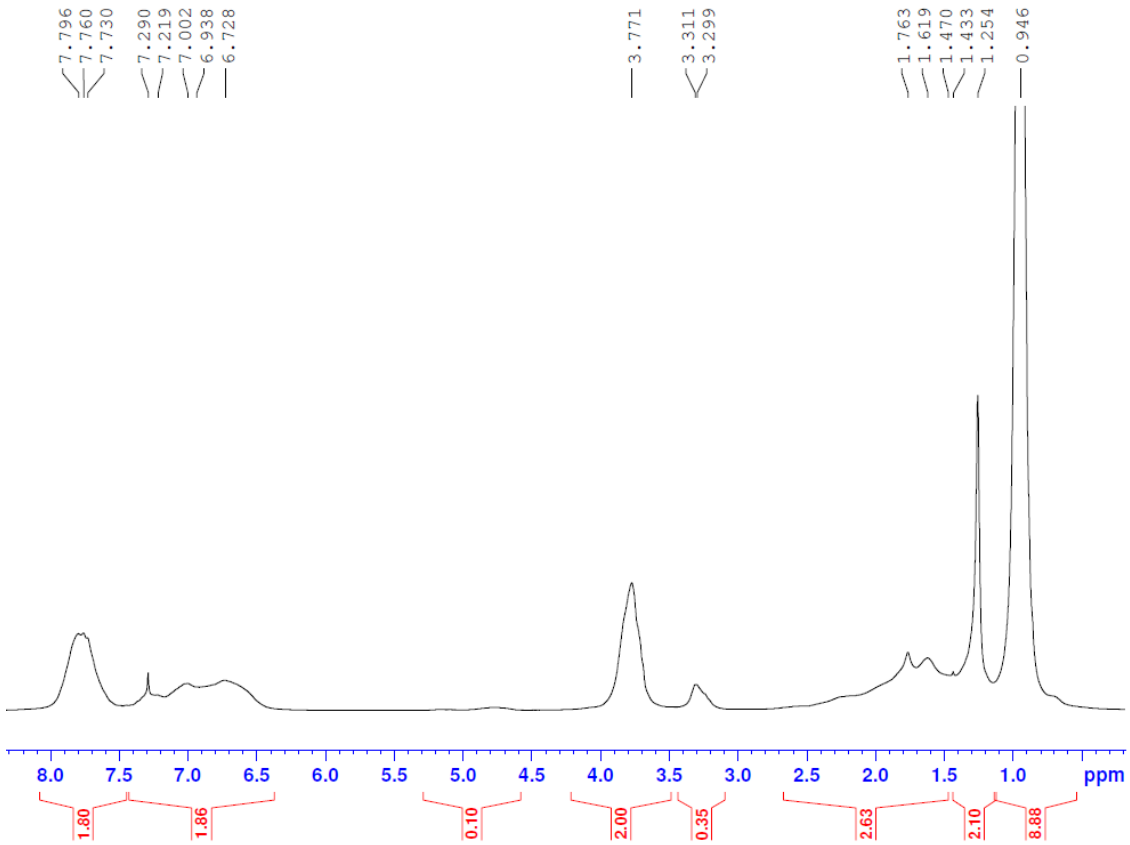

Figure S3. ^{1}H NMR spectrum of $PNSS_{9}$-N_3.

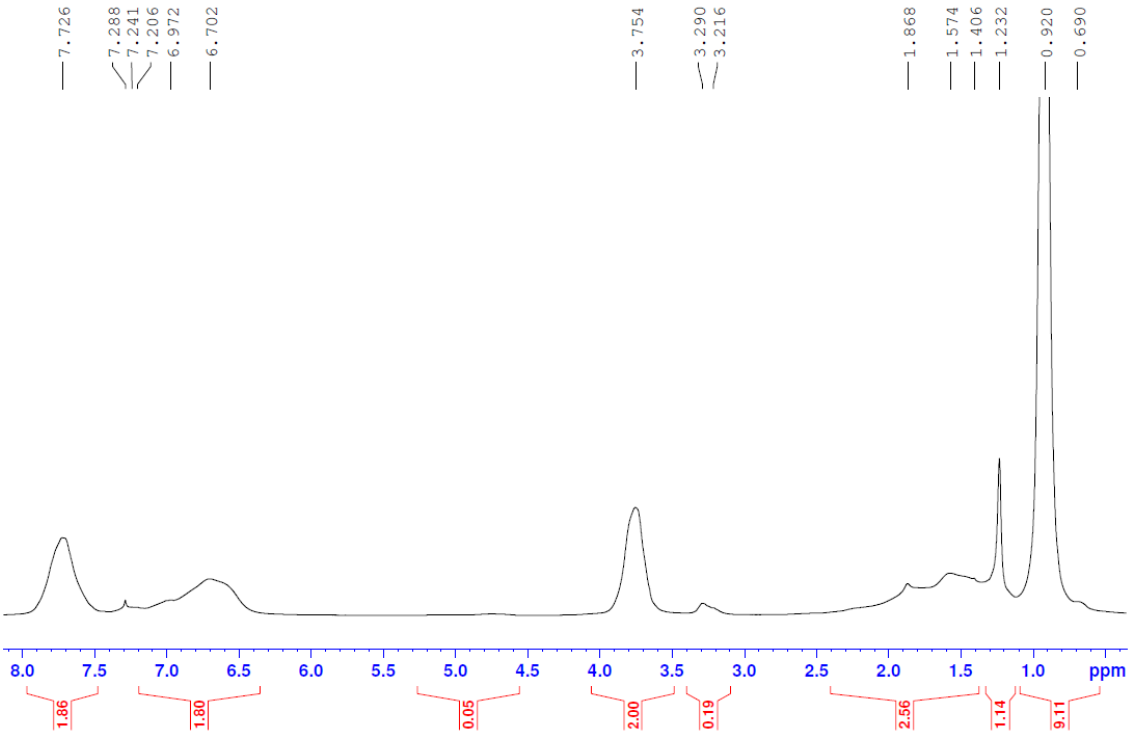

Figure S4. ^{1}H NMR spectrum of $PNSS_{16}$-N_3.

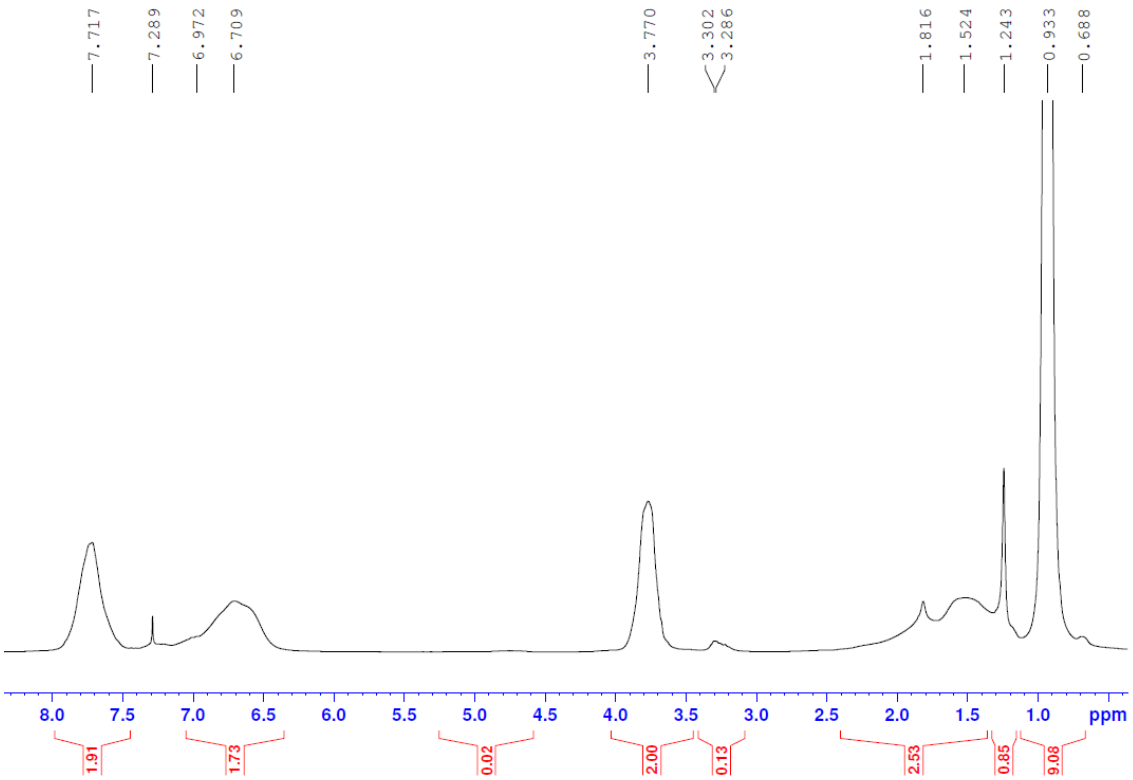

Figure S5. ^{1}H NMR spectrum of $PNSS_{23}$-N_3.

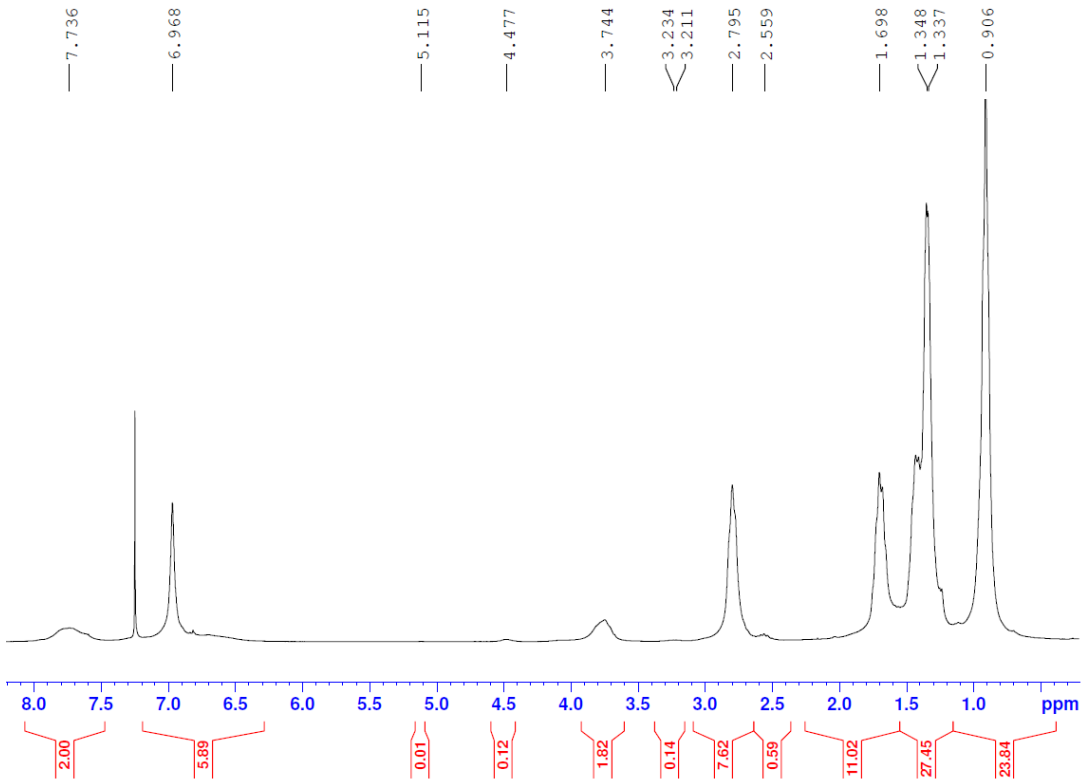

Figure S6. ^{1}H NMR spectrum of $P3HT_{50}$-*b*-$PNSS_9$.

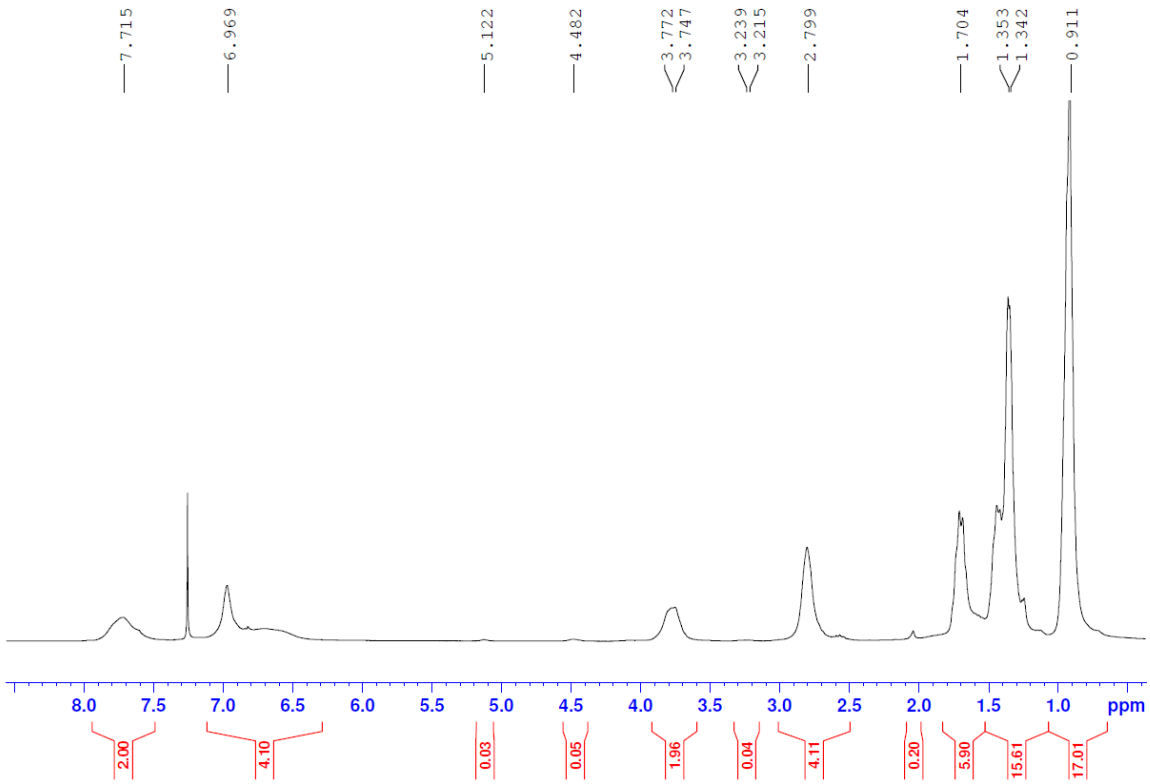

Figure S7. ^{1}H NMR spectrum of P3HT$_{50}$-*b*-PNSS$_{16}$.

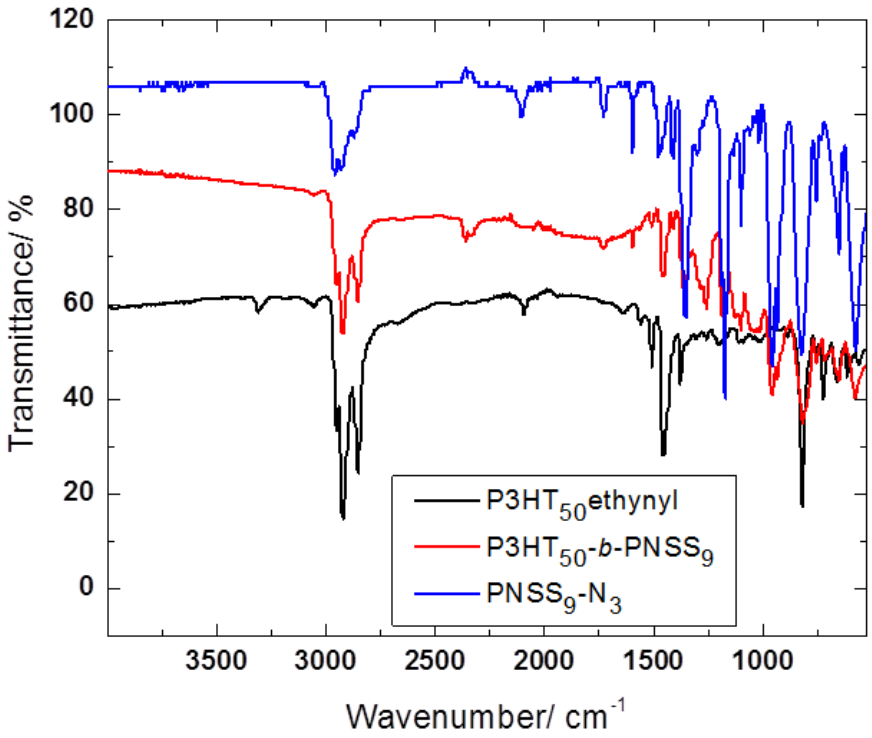

Figure S8. FTIR spectra of P3HT$_{50}$-*b*-PNSS$_{9}$, P3HT$_{50}$-ethynyl and PNSS$_{9}$-N$_{3}$.

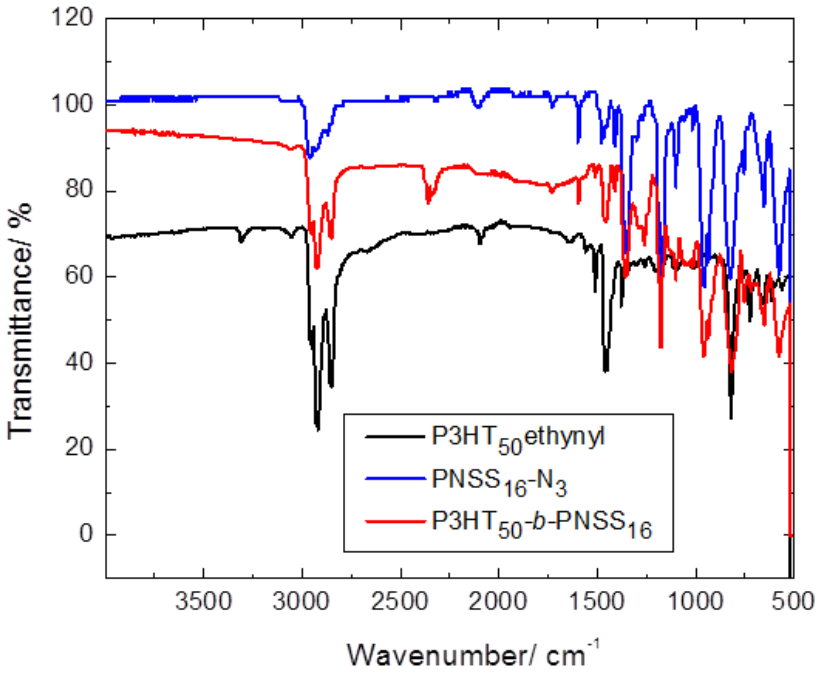

Figure S9. FTIR spectra of $P3HT_{50}$-*b*-$PNSS_{16}$, $P3HT_{50}$-ethynyl and $PNSS_{16}$-N_3.

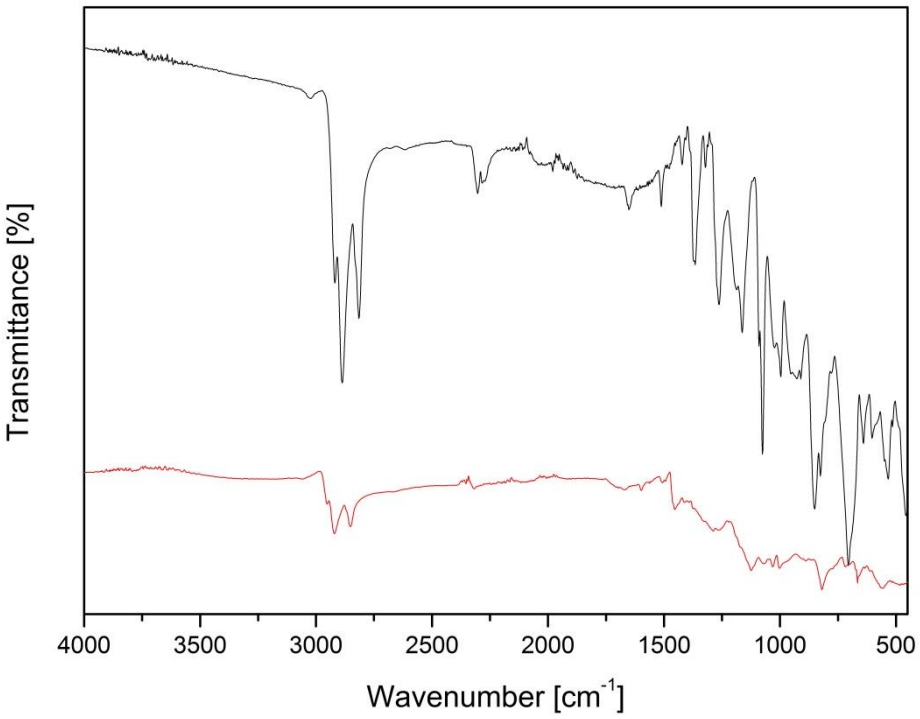

Figure S10. FTIR spectra of $P3HT_{50}$-*b*-$PNSS_9$ before (top) and after (bottom) thermal treatment (3 hours at 150 °C). The spectra have been translated along the transmission axis for clarity purposes.

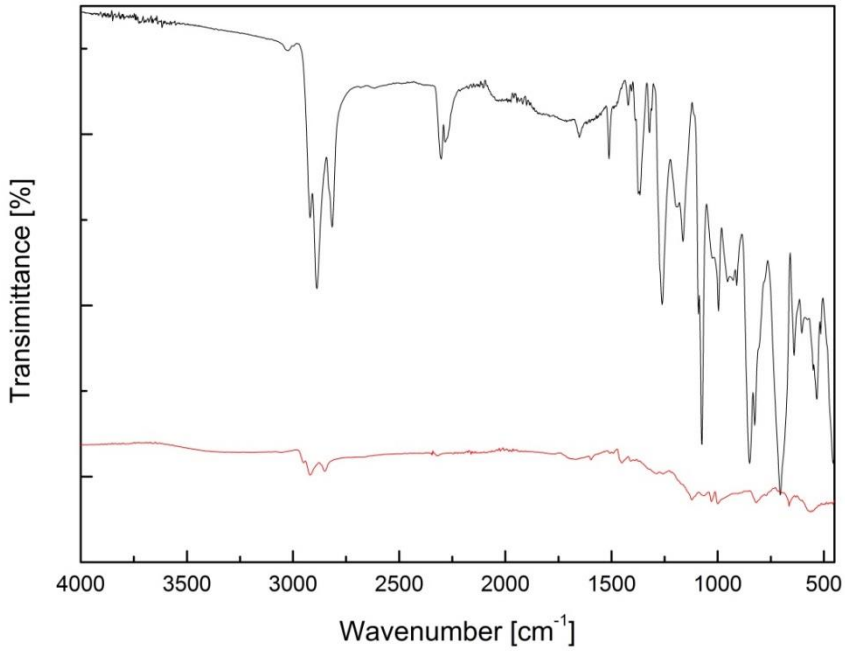

Figure S11. FTIR spectra of $P3HT_{50}$-*b*-$PNSS_{16}$ before (top) and after (bottom) thermal treatment (3 hours at 150 °C). The spectra have been translated along the transmission axis for clarity purposes.

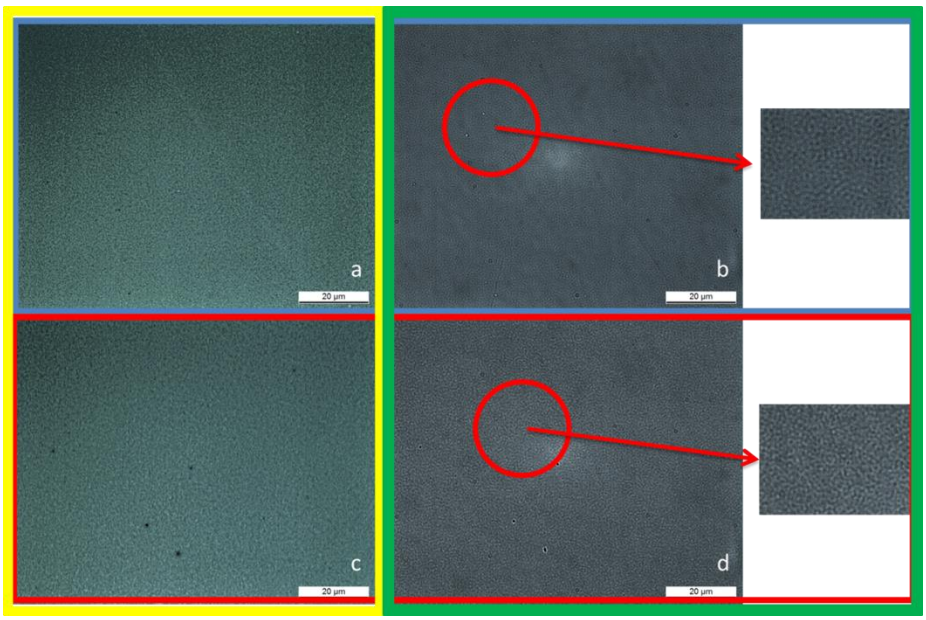

Figure S12. Optical microscopy images of $P3HT_{50}$-*b*-$PNSS_9$ as (a) the pristine film in reflection mode; (b) the pristine film in transmission; (c) after thermal treatment/deprotection in reflection mode; and (d) after thermal treatment/deprotection in transmission mode. These images are representative of all of our block copolymers.

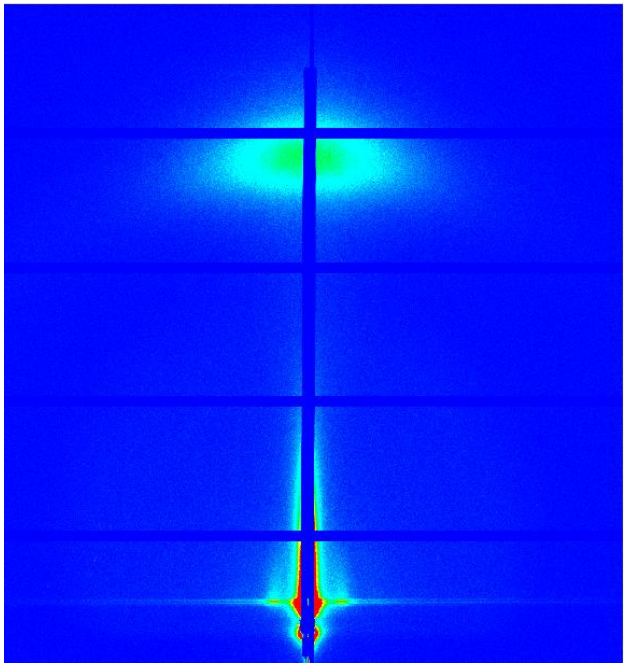

Figure S13. Raw 2D GISAXS/GIWAXS image for $P3HT_{50}$ homopolymer annealed for 3 hours at 150 °C, showing a weak SAXS peak just over 17 nm and WAXS peak at ca. 1.6 nm.

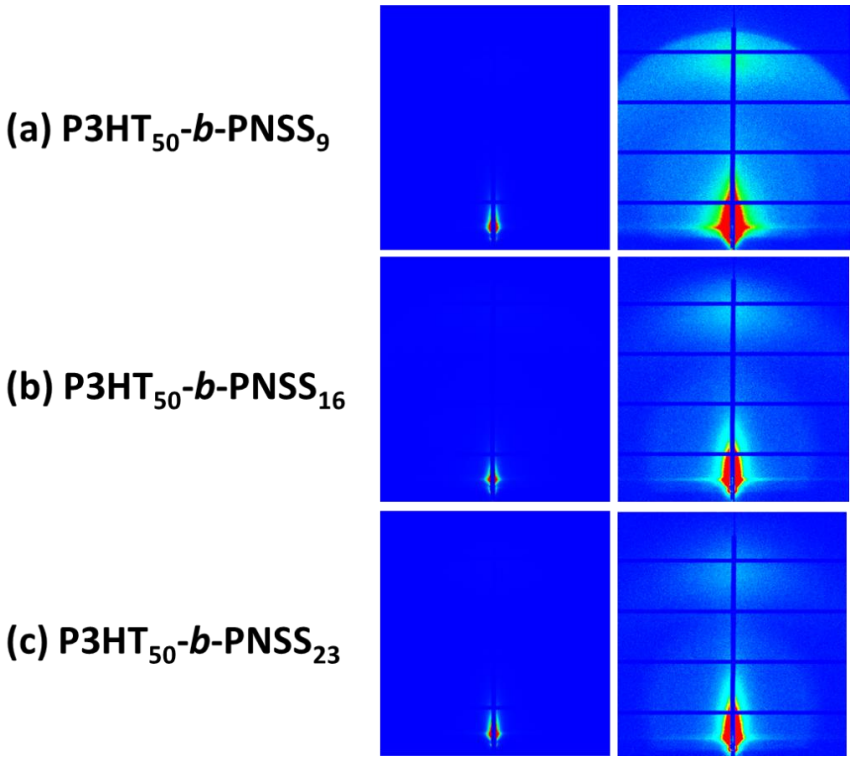

Figure S14. Raw 2D GISAXS/GIWAXS images for (a) $P3HT_{50}$-*b*-$PNSS_9$, (b) $P3HT_{50}$-*b*-$PNSS_{16}$ and (c) $P3HT_{50}$-*b*-$PNSS_{23}$ block copolymers after solvent annealing in THF atmosphere for 36 hours. The images on the right hand side are at enhanced intensity to accentuate the WAXS feature.

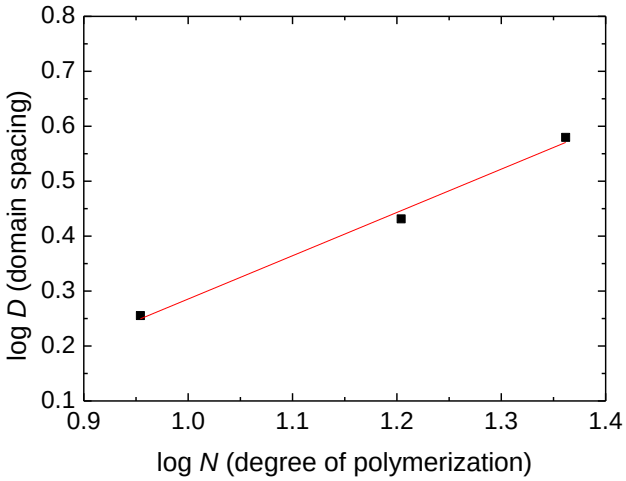

Figure S15. Plot of log *D* versus log *N* for the amorphous PSS domains in the block copolymer series, P3HT$_{50}$-*b*-PSS$_{9}$, P3HT$_{50}$-*b*-PSS$_{16}$ and P3HT$_{50}$-*b*-PSS$_{23}$. N.B. Caution should be taken when using these values as our TGA data show that the shorter PNSS blocks have only been partially thermolyzed and therefore the volume occupied by the repeat unit will be moderately different.

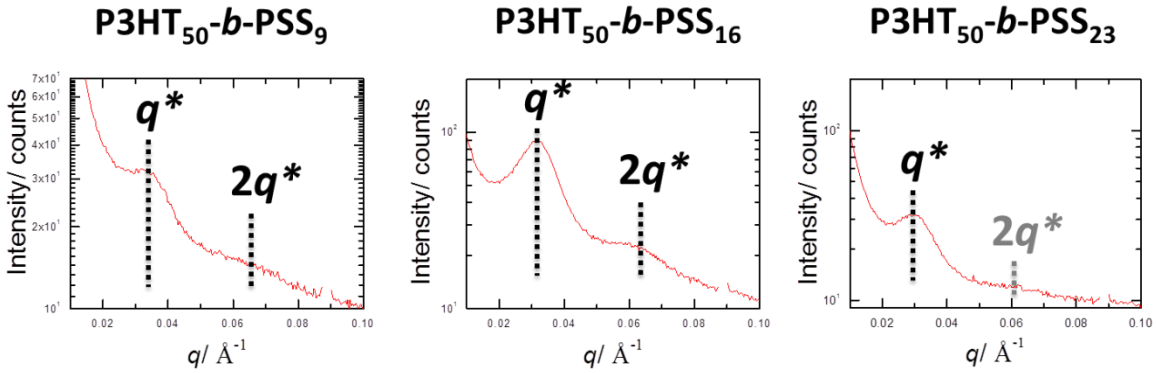

Figure S16. 1D GISAXS profiles for the diblock copolymers following thermolysis at 150 °C for 3 hours. These data are taken from Figure 6 of the main manuscript to highlight the second order Bragg peaks in each case.

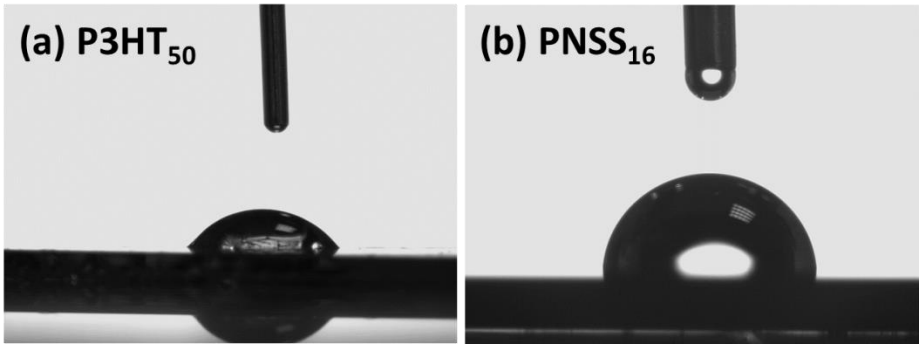

Figure S17. Contact angle images for (a) $P3HT_{50}$alkyne (55 °) and (b) $PNSS_{16}N_3$ (98 °) homopolymers.

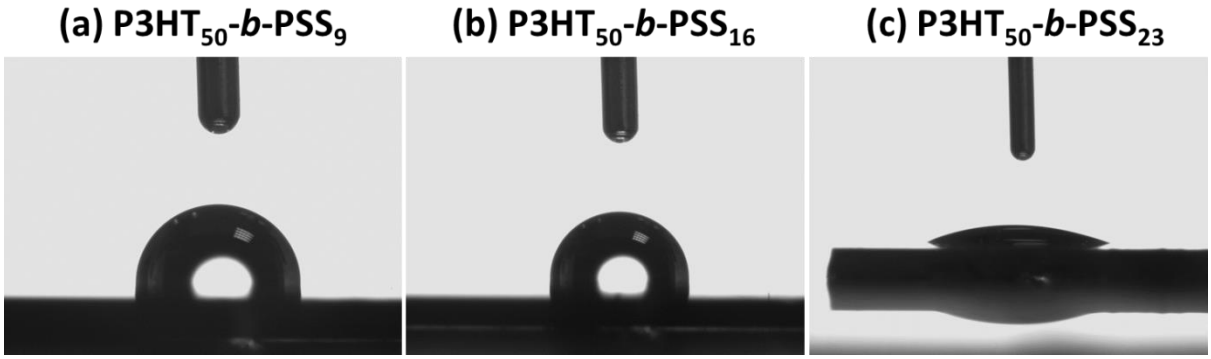

Figure S18. Contact angle images of the block copolymers after 3 hours annealing at 150 °C; (a) $P3HT_{50}$-*b*-PSS_9 (93 °); (b) $P3HT_{50}$-*b*-PSS_{16} (95 °) and (c) $P3HT_{50}$-*b*-PSS_{23} (21 °).

As shown in Figure S14, the contact angle images of the homopolymer films, $P3HT_{50}$ and $PNSS_{16}N_3$, show that PNSS (contact angle of 98 °) is more hydrophobic than P3HT (contact angle of 55 °), due to higher surface energy of PNSS in comparison to P3HT (26.9 mN/m).[1] Following deprotection (thermal treatment at 150 °C for 3 hours), the contact angles of the block copolymers with the low PNSS content do not change significantly (due to partial deprotection of the PNSS blocks), whereas $P3HT_{50}$-*b*-$PNSS_{23}$ is fully deprotected to $P3HT_{50}$-*b*-PSS_{23}, giving a dramatically lower contact angle. Thermodynamically, it is more favourable that the lowest surface energy polymer will migrate to air/active layer interface, during thermal annealing, in order to reduce the overall energy of the system. Therefore the lack of lateral phase separation on the surface could be related to formation of a wetting layer of one of the polymer blocks (the extent of deprotection determining which block preferentially forms the surface skin). The formation of such wetting layers has been previously seen in other block copolymer systems.[2,3] To study the buried structure beneath the wetting layer, the wetting layer was removed by exposing the films to UV/ozone for varying times, using a Novascan PSD PRO-UV ozone generator. The process was optimised for each sample. Figure S16 shows the

AFM topography images, revealing phase separated domains after removal of the wetting layer. The domain spacing for P3HT$_{50}$-*b*-PNSS$_{16}$ from the Fast Fourier Transform (FFT) is 19.8 nm, giving good agreement with the GISAXS measurement of 19.7 nm. However, the domain spacing for P3HT$_{50}$-*b*-PNSS$_{9}$ and P3HT$_{50}$-*b*-PNSS$_{23}$ could not be read from FFT due to background noise. As an alternative, line profiling was used from the topographic images to reveal approximate domain spacings of 29 nm and 30 nm, respectively, while the GISAXS measurements give 18.8 nm and 20.8 nm. This difference is attributed to the approximation in the calculation arising from the noisy images and the structure not being completely perpendicular to the surface, which would alter the perceived spacing observed from above.

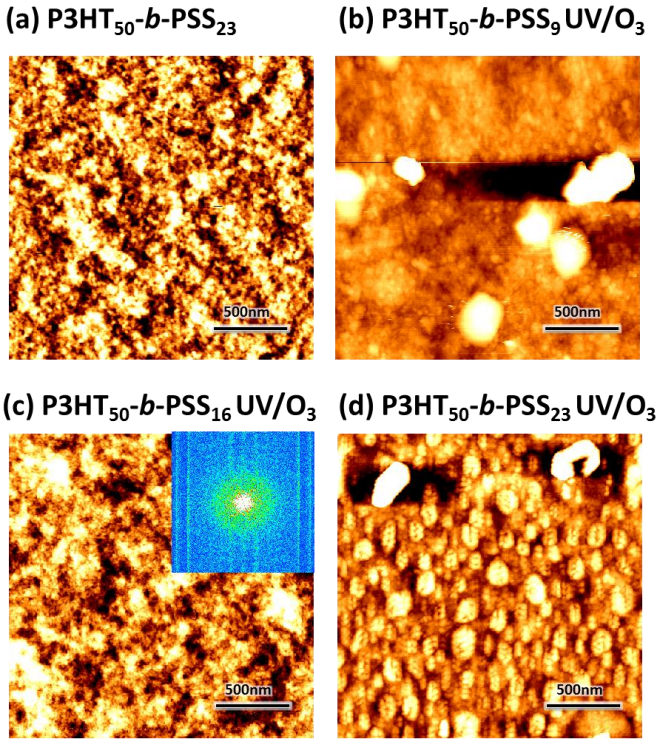

Figure S19. AFM topography images of; (a) P3HT-*b*-PSS$_{23}$ after thermal annealing at 150 °C for 3 hours and before removal of the wetting layer by UV/ozone; (b) P3HT-*b*-PSS$_{9}$ after thermal annealing and UV/O$_3$ exposure for 7 minutes; (c) P3HT-*b*-PSS$_{16}$ after thermal annealing and UV/O$_3$ exposure for 10 minutes (with FFT inset) and (d) P3HT-*b*-PSS$_{23}$ after thermal annealing and UV/O$_3$ exposure for 3 minutes.

(1) Germack, D. S.; Chan, C. K.; Hamadani, B. H.; Richter, L. J.; Fischer, D. A.; Gundlach, D. J.; DeLongchamp, D. M. *Applied Physics Letters* **2009**, *94*.

(2) O'Driscoll, B. M. D.; Kelly, R. A.; Shaw, M.; Mokarian-Tabari, P.; Liontos, G.; Ntetsikas, K.; Avgeropoulos, A.; Petkov, N.; Morris, M. A. *European Polymer Journal* **2013**, *49*, 3445.

(3) Archambault, S.; Girardot, C.; Salaün, M.; Delalande, M.; Böhme, S.; Cunge, G.; Pargon, E.; Joubert, O.; Zelsmann, M. 2014; Vol. 9054, p 90540O.